Electronic Supplementary Material (ESI) for Physical Chemistry Chemical Physics.

Supplementary Information for

Revisit of the Plasmon-Mediated Chemical Transformation of para-Aminothiophenol

Toshiki Kondo,[1] Motoharu Inagaki,[1] Shohei Tanaka,[2] Shinya Tsukiji,[2,3] Kenta Motobayashi,[1] and Katsuyoshi Ikeda[,1,4]*

[1]Department of Physical Science and Engineering, Nagoya Institute of Technology, Nagoya 466-8555, Japan.

[2]Department of Life Science and Applied Chemistry, Nagoya Institute of Technology, Nagoya 466-8555, Japan.

[3]Department of Nanopharmaceutical Sciences, Nagoya Institute of Technology, Nagoya 466-8555, Japan.

[4]Frontier Research Institute for Materials Science (FRIMS), Nagoya Institute of Technology, Nagoya 466-8555, Japan.

*Corresponding Authors: kikeda@nitech.ac.jp

1. Low-frequency vibrational analysis in SERS spectroscopy

Figure S1(a) shows a typical SERS spectrum for pATP monolayers on Au in a wide range of frequencies covering both Stokes and anti-Stokes branches. It is known that SERS spectrum is accompanied with a background continuum. Unfortunately, this background dominates in the low-frequency region below 200 cm^{-1}, which is problematic in analyzing low-frequency vibrations. Recently, we have found that the origin of the background can be well explained by plasmon-enhanced electronic Raman scattering, which allowed us to convert measured SERS spectrum to a density of states format by reducing the Bose-Einstein thermal factor, frequency factor, and the Purcell factor. Figure S1(b) shows the reduced form of (a), in which the symmetry of the spectral features between Stokes and anti-Stokes branches indicates that the vibrational information was properly extracted from the measured spectrum. It is clear that the reduced spectrum is favorable for analyzing low-frequency region especially in the THz-shifted region. The detailed procedure was reported elsewhere.[45-48]

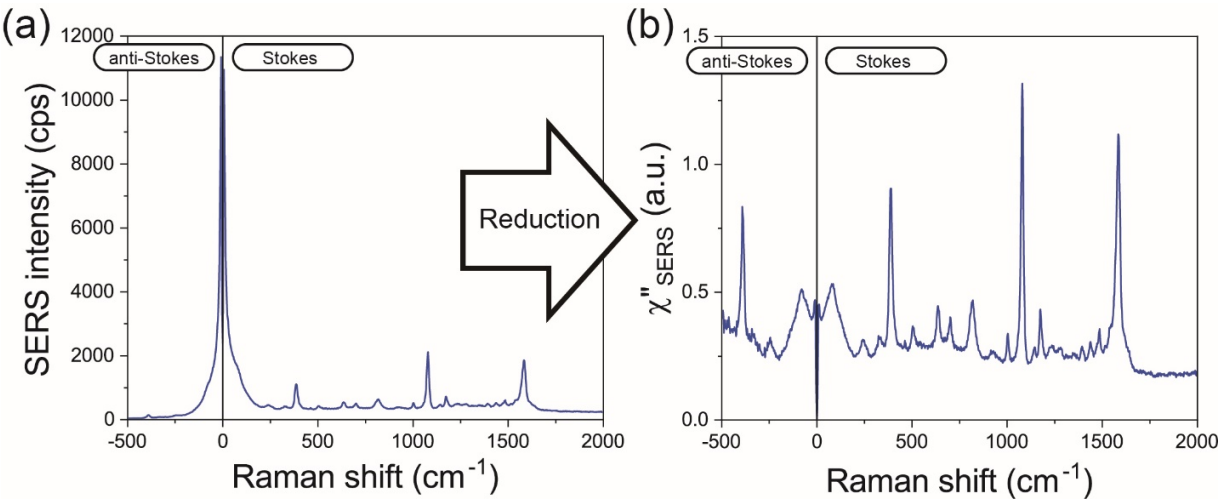

Figure S1. (a) a typical measured SERS spectrum for pATP monolayers on Au. (b) a density of states format of (a) obtained by reducing thermal, frequency, and Purcell factors.

2. SERS spectra of pATP and *trans*-DMAB

Figure S2 shows linear sweep voltammograms of pATP on Au(111) and Au(100) in 0.1 M KOH aqueous solution. The reductive desorption of pATP molecules is observed as a peak at around −0.64 V on Au(111) and −0.85 V on Au(100). This difference is dominantly dependent on the surface energy of Au substrate. On the other hand, the difference in the surface atomic arrangements between (111) and (100) lead to the different Au-S bond configuration; the dominant Au-S bond is in the hollow configuration on Au(111) and the bridge configuration on Au(100). This can be confirmed by the frequency of Au-S stretching mode because the frequency of surface-adsorbate stretching mode decreases with increasing ligancy at the adsorption sites.[63] Importantly, the different adsorption configuration is accompanied by the different orientation of adsorbed molecules on the surface. Thus, pATP molecules stand almost upright on the hollow sites while lying flat on the bridge sites. Because the degree of the resonance transition is changed by the molecular orientation, the b2 modes of pATP gain more intensity in the hollow configuration.

The above description about the different adsorption configurations of pATP between Au(111) and Au(100) is indeed observed in SERS spectra of pATP. When the nanoparticle-on-mirror (NPoM)-based SERS spectroscopy is conducted on Au(111) and Au(100) covered with pATP, the frequency of νAu-S is slightly lower on Au(111) than on Au(100), as shown in the upper panel of Fig. S3, indicating the crystallographic orientation-dependence in the ligancy of S atoms on Au surface. (It is noted that other benzenethiol derivatives like 4-methylbenzenethiol showed much clearer difference in the frequency of νAu-S.[44]) Moreover, this configurational difference between Au(111) and Au(100) is consistent with the fact that the relative intensities of the b2 modes are much larger on Au(111) than on Au(100). On the other hand, SERS spectrum

of *trans*-DMAB is similar between Au(111) and Au(100), as shown in the bottom panel of Fig. S3. (In the case of DMAB with two thiol anchor groups, it is difficult to distinguish the difference in the adsorption sites between Au(111) and Au(100) because one of the S atoms is adsorbed on Au nanoparticles.)

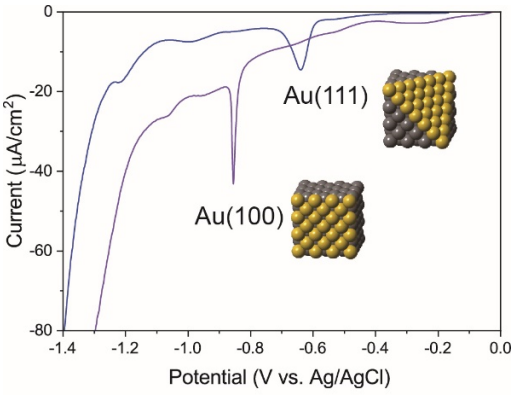

Figure S2. Different reductive desorption behaviors of pATP on Au(111) and Au(100), measured using the negative-going linear sweep voltammetry in 0.1 M KOH aqueous solution with the scan rate of 20 mV/s.

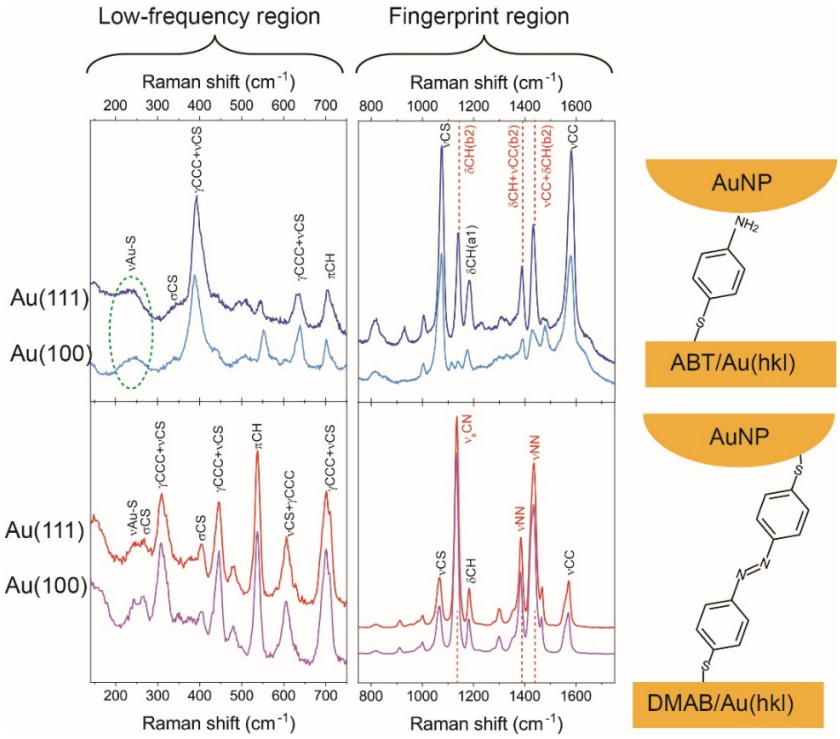

Figure S3. (Upper panel) SERS spectra of pATP measured on Au(111) and Au(100). (Bottom panel) SERS spectra of trans-DMAB measured on Au(111) and Au(100). Au nanoparticles with diameter of 50 nm were adsorbed on top of monolayers to increase Raman scattering signals.

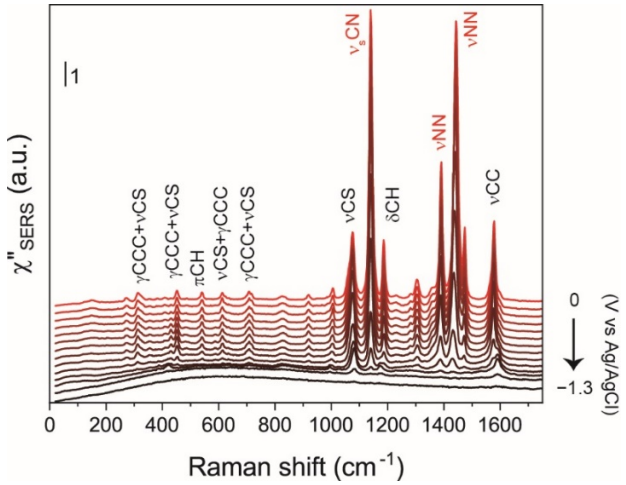

Figure S4. Potential dependent SERS spectra of *trans*-DMAB on rough Au measured in 0.1 M KOH aqueous solution under the negative-going scan. A zoom-out view of Fig. 6b.

3. DFT calculations of Raman spectra of adsorbates

The assignment of fingerprint vibrational peaks in SERS spectra were conducted by assistance of the density functional theory (DFT) calculations of Raman spectra for different benzenethiol derivatives on an Au cluster, which were performed using Gaussian 09, revision A02, at the B3LYP level of theory with the LanL2DZ basis set for the Au atoms and 6-31G** basis sets for other atoms of neutral species. The vibrational scaling factor used was 0.961 for 6-31G**. The tetrahedral cluster of Au_{20} was used as a substrate in the calculation because this structure, *i.e.*, a fragment of the face-centered cubic lattice of bulk gold with a small structural relaxation, is a minimum cluster which enables the adsorption of DMAB in the *cis*-configuration. As shown in Fig. S5, frequencies of the fingerprint vibrations are insensitive to the cluster sizes, meaning that the size of the cluster do not affect much the vibrational assignment in the fingerprint region. For Au-S bonds, the bridge configuration was assumed because the hollow configuration was not optimized without considering van der Waals interactions between molecules. In the calculated results in Figs. S6 - S8, vibrational assignments, determined by visualization of the calculated vibration modes, are indicated in the entire frequency range, but the comparison of the calculated results with the measured spectra was conducted in the fingerprint region above 800 cm^{-1}.

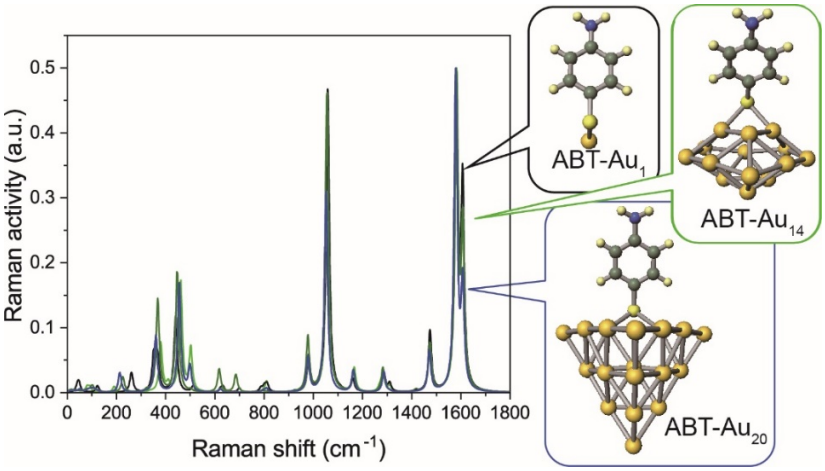

Figure S5. Cluster size dependence of calculated Raman spectra for ABT attached onto Au_n clusters (n = 1, 14, and 20).

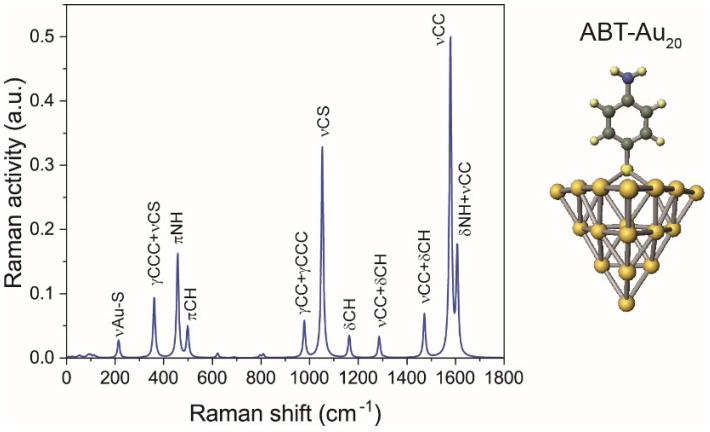

Figure S6. Calculated Raman spectrum for pATP attached onto an Au_{20} cluster.

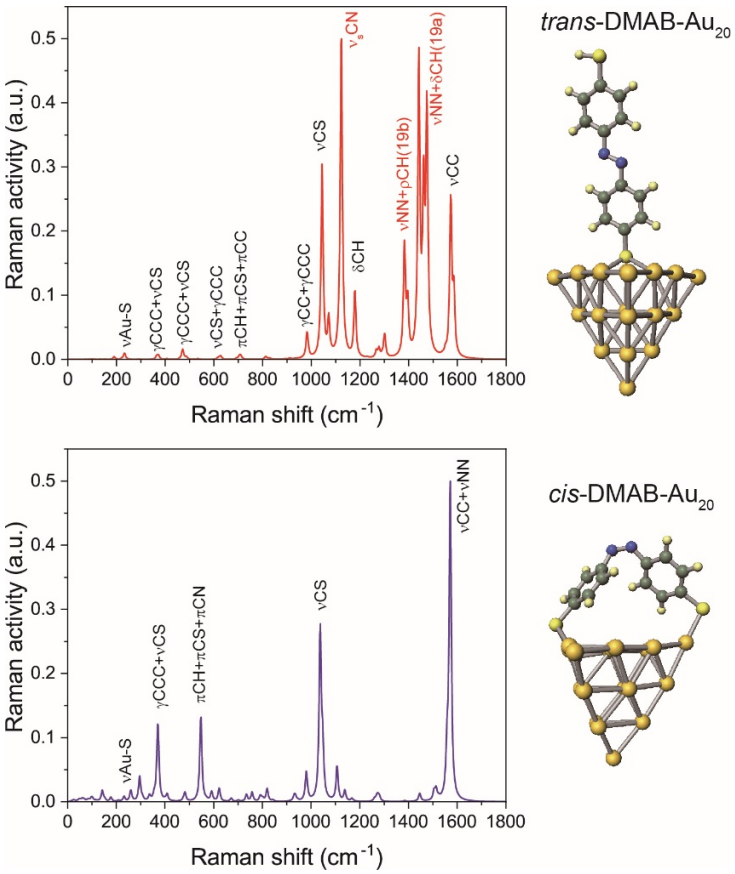

Figure S7. Calculated Raman spectra for *trans*-DMAB and *cis*-DMAB attached onto an Au_{20} cluster.

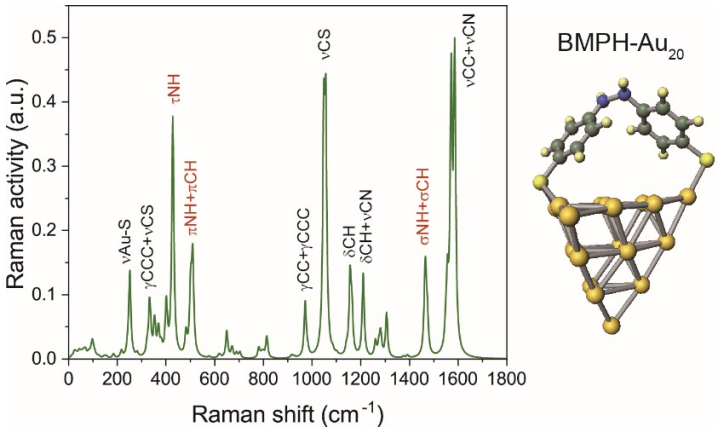

Figure S8. Calculated Raman spectrum for BMPH attached onto an Au_{20} cluster.